Mini-Emulsion Polymerized Poly(Urethane-Urea)/CoFe$_2$O$_4$ Nanocomposite: Structural Characterization and Application in Dye Removal from Water

M. P. Varshini[1], S. Vennila[2], and G. Sankar[1]*

[1]Department of Polymer Science, University of Madras, Guindy Campus, Chennai, Tamil Nadu, India, [2]Key Laboratory of State Forestry Administration for Silviculture of the Lower Yellow River, College of Forestry, Shandong Agricultural University, Taian, China

ABSTRACT

Synthesized a reusable, cost-effective poly(urethane-urea) (PUU)/CoFe$_2$O$_4$ (PUU/magnetic nanoparticle [MNp]) magnetic nanocomposite for the efficient removal of crystal violet (CV) dye from aqueous media. CoFe$_2$O$_4$ MNps were prepared through the co-precipitation method and subsequently embedded into a PUU matrix through mini-emulsion polymerization to minimize nanoparticle agglomeration. Performed structural characterization using attenuated total reflectance Fourier-transform infrared spectroscopy and X-ray diffraction. Evaluated dye removal performance using Ultraviolet-visible spectroscopy and varied parameters, such as dye concentration, nanocomposite dosage, contact time, and pH. The synthesis process was environmentally benign and non-toxic, yielding a material with high recyclability. The nanocomposite showed rapid adsorption capabilities, achieving approximately 98–100% degradation of 100 ppm CV within 90 min. These results highlight the potential applicability of the PUU/MNp nanocomposite in wastewater treatment systems targeting synthetic dye pollutants.

Key words: CoFe$_2$O$_4$ magnetic nanoparticle, Crystal violet dye, Mini emulsion polymerization, Nanocomposite, Poly(urethane-urea)PUU/CoFe$_2$O$_4$, Ultraviolet-visible spectroscopy.

1. INTRODUCTION

Dyes are chemical substances that bond with the surfaces of fabrics to impart color. Most dyes possess chemically complex molecular structures and resist several degrading factors, including detergent activity [1]. The leather, paper, and textile industries extensively employ synthetic dyes, which are typically non-biodegradable and toxic, for coloration. Globally, textile industries account for the use of approximately 10,000 tons of dyes annually, among other dye-used sectors [2]. Even trace amounts of dyes introduced into water bodies are visibly detectable and can significantly disrupt aquatic ecosystems by causing harm to aquatic organisms [3]. The presence of synthetic dyes in soil or water resources may interfere with the food chain and reduce soil fertility, raising concerns regarding food safety. Improperly disposed dye wastes are highly carcinogenic, contributing to respiratory ailments, such as asthma, as well as skin irritations and allergic reactions [4].

A vast number of dye types are currently in use worldwide. Among these, azo dyes form a prominent category of organic dyes, widely produced and used across industries. Azo dyes, which contain an azo functional group (-N=N-), represent one of the oldest classifications of synthetic dyes. Globally, approximately 3,000 varieties of azo dyes are in circulation, extensively used in textile processing [5]. However, the discharge of these dyes into aqueous environments has led to significant environmental concerns because of their toxicity and persistence. Effective removal of these dyes from contaminated water is critical for environmental sustainability [6].

Various chemical treatment techniques are available for dye removal, using materials, such as alum, activated carbon, and ferric chloride. However, these methods are often costly and cannot achieve effective dye degradation [7]. In response to these challenges, the present study introduces cobalt ferrite (CoFe$_2$O$_4$) magnetic nanoparticles (MNPs) as a promising alternative. While studies explored other MNPs for dye degradation, CoFe$_2$O$_4$ demonstrates superior performance because of its magneto-resistive and magneto-optical properties, low cost, and enhanced efficiency in dye removal [8]. Despite these advantages, CoFe$_2$O$_4$ nanoparticles are prone to aggregation in solution, which limits their surface accessibility and dye degradation efficiency [9].

To address this limitation, the super-paramagnetic properties of CoFe$_2$O$_4$ nanoparticles can be stabilized through incorporation into polymeric matrices, preventing agglomeration and enhancing reactivity. In this work, we incorporated CoFe$_2$O$_4$ MNPs into a poly(urethane-urea) (PUU) matrix. We used interfacial step-growth polymerization in mini-emulsion, with 1,4-butanediol and hexamethylene diisocyanate as pre-cursors [10]. Previous studies reported incorporating metal nanoparticles into various polymer systems [11-13], but, to our knowledge, no one has yet reported the synthesis of CoFe$_2$O$_4$ nanoparticles embedded

GRAPHICAL ABSTRACT
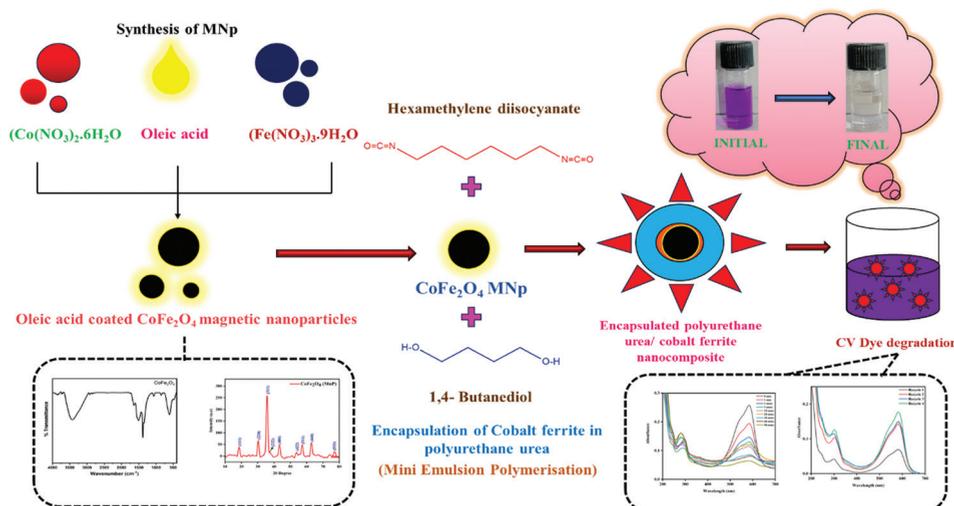
in linear PUU for crystal violet (CV) dye degradation. We used the resulting PUU/MNP nanocomposite to investigate CV dye adsorption, evaluating the effects of initial dye and nanoparticle concentrations, contact time, pH, and material recyclability.

2. EXPERIMENTAL SECTION

2.1. Materials and Methods

Cobaltous nitrate hexahydrate ($Co(NO_3)_2.6H_2O$; S.D Fine Chem Ltd, Chennai, India), Concentrated Hydrochloric Acid (Con. HCL; Fisher Scientific, Chennai, India), Ferric Nitrate ($Fe(NO_3)_3.9H_2O$; S.D Fine Chem Ltd., Chennai, India), Sodium Hydroxide (NaOH; SRL, Chennai, India), Ethanol (EtOH; Analytical CSS reagent, Chennai, India), 1,4 Butanediol (Loba Chemie, Chennai, India), Sodium dodecyl sulfate (SDS; SRL, Chennai, India), Hexamethylene Diisocyanate (HDI; TCI, Chennai, India), Oleic Acid (OA; TCI, Chennai, India), Cyclohexane (TCI, Chennai, India) were purchased and used.

2.2. Measurements

Initially, the structure of the synthesized compound was determined by Fourier-transform infrared spectroscopy (FTIR). Using a Nicolet iS50 FTIR (Thermo Nicolet, Chennai, India), we conducted the FTIR analysis. The Nicolet iS50 FTIR had attenuated total reflectance (ATR) mode. Performed powder X-ray diffraction (XRD) studies of $CoFe_2O_4$ using a Bruker D2 PHASER (Taipei, Taiwan) diffractometer. The diffractometer operated at 30 kV with a Cu Kα ($\lambda = 0.15418$ nm) target and had an angular range from 10 to 80° (2Θ). CV dye degradation analysis followed using a Perkin Elmer Lambda-650 liquid Ultraviolet (UV)-visible spectrophotometer (Chennai, India).

2.3. Synthesis of OA Coated $CoFe_2O_4$ MNPs

The co-precipitation method is one of the best methods for the synthesis of MNPs, having a significant advantage of producing the MNPs in larger amounts compared to other methods [14]. Here, this method was used to synthesize OA coated $CoFe_2O_4$ MNPs by adding Cobaltous nitrate hexahydrate and ferric nitrate as pre-cursors in a 1:2 molar ratio. In one beaker, 10 mmol of Co ($NO_3)_2 \cdot 6H_2O$ was combined with 4 mL of deionized water. Simultaneously, in another beaker, 1 mL Con.HCl, 20 mmol of Fe ($NO_3)_3.9H_2O$, 40 mL of de-ionized water, and 3 mL of OA were added. The two solutions were kept at 50°C for 30 min under constant stirring. Then, the mixture of Co ($NO_3)_2 \cdot 6H_2O$ and Fe

($NO_3)_3 \cdot 9H_2O$ was added drop-wise to 200 mL of 1 M NaOH, kept stirring continuously at 100°C for 1 h. A gray solution was observed, along with the precipitation of magnetic nanoparticles (MNPs). After cooling, the solution was allowed to well settle. Using a permanent magnet, removed the precipitate to eliminate pre-cursor nitrate or ions and OA. Then, we washed the precipitate with distilled water and ethanol. A vacuum desiccator at room temperature was used to dry the obtained MNP.

2.4. Encapsulation of $CoFe_2O_4$ MNPs in PUU through Mini-Emulsion Polymerization

MNPs' strong tendency to agglomerate requires protection by grafting or coating with organic species, surfactants, or polymers [15]. Using HDI (diisocyanate) and 1,4-Butanediol as monomers, OA (17%) as a co-stabilizer, and SDS (3%) as a surfactant, produced 10% MNPs. The organic phase contains (HDI, cyclohexane, OA, and $CoFe_2O_4$) and the aqueous phase (1,4-butanediol, water, and SDS) were thoroughly mixed for 20 min in a magnetic stirrer. After 20 min, sonicated the formed coarse material for about 3 min. Then, transferred the mixture into a round-bottom flask and kept it for polymerization at 70°C for 3 h. Washed the formed oily precipitate with distilled water and then dried it in a vacuum desiccator at room temperature.

2.5. Stock Solution Preparation of CV for Dye Degradation

Prepared the stock solution by dissolving 50 mg of CV in 500 mL of deionized water. Then, diluted the stock solution to create five dye solutions of different concentrations (10, 30, 50, 70, and 100 ppm). These different concentrations were used to analyze the effects of initial dye concentration on the dye adsorption using 50 mg of $CoFe_2O_4$ MNp encapsulated in PUU to produce a nanocomposite. A 100 ppm concentrated dye solution was used to analyze the effects of time, pH, and MNp concentration variations.

3. RESULT AND DISCUSSION

3.1. Literature Review of Dye Adsorption using Different MNPs

The comparative literature review of dye adsorption using various magnetic nanoparticle-based composites were given in Table 1. It highlights the pH ranges, contact times, and recyclability characteristics across different adsorbents.
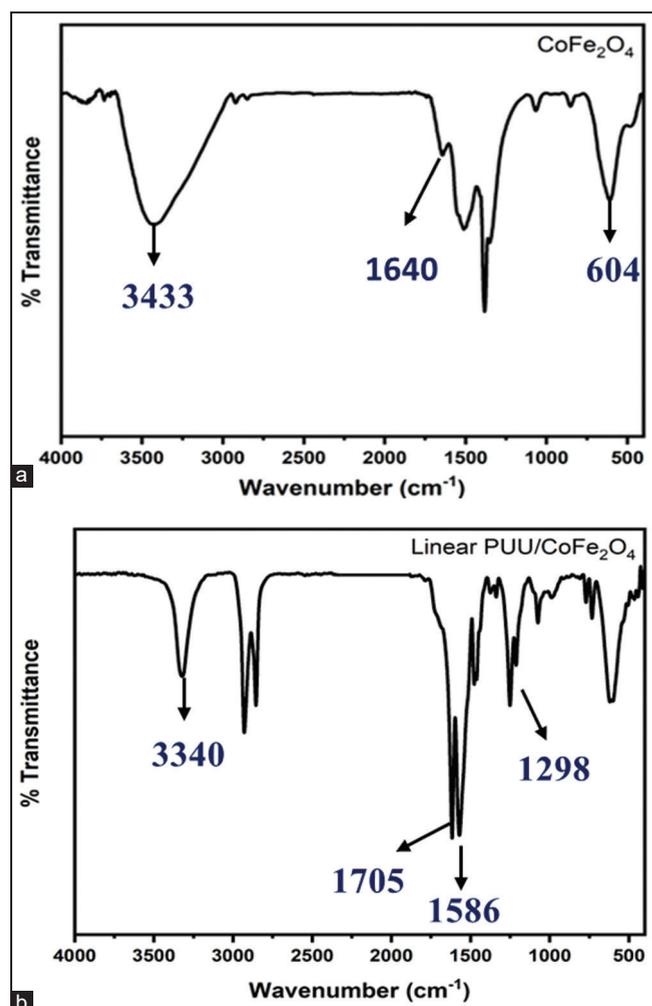
Figure 1: ATR-Fourier-transform infrared spectroscopy analysis of $CoFe_2O_4$ (a) and poly(urethane-urea)/$CoFe_2O_4$ (b) MNp.

Figure 2: X-ray diffraction pattern of $CoFe_2O_4$ nanoparticles.

Table 1: Literature review of dye adsorption using different magnetic nanoparticles.

S. No.	Polymeric magnetic Nanocomposite	Experimental conditions	References
1	$Fe_3O_4@$- PANI	pH – 1–9 Time – 5 min–4 h	[16]
2	Gg-cl-P (AA-co-AAm)/Fe_3O_4	pH – 2–11 Time – 0–240 min Recyclability – three cycles	[17]
3	CMC-coated $Fe_3O_4@$ SiO_2 MNPs	pH – 3–11 Time – 0–180 min	[18]
4	Sulfonated waste polystyrene with $CoFe_2O_4$ MNp	Time – 5 min–48 h Recyclability – four cycles	[19]
5	PUU/$CoFe_2O_4$	pH – 1–11 Time – 0–90 min Recyclability – four cycles	This work

PUU: Poly (urethane-urea), MNp: Magnetic nanoparticle

3.2. Structural Characterization of PUU/MNp

The ATR-FTIR spectra presented in Figure 1a confirm the characteristic vibrational bands of $CoFe_2O_4$. The peaks observed at 604 cm^{-1}, 3433 cm^{-1}, and 1640 cm^{-1} correspond to Fe–O vibrations and O–H stretching modes, indicating hydroxyl groups adsorbed on the surface of the $CoFe_2O_4$ nanoparticles [20]. In Figure 1b, the infrared spectrum of the PUU/$CoFe_2O_4$ (PUU/MNp) nanocomposite exhibits a prominent peak at 3340 cm^{-1}, attributed to N–H stretching vibrations, suggesting urethane bond formation. The C=O stretching vibration of the urethane groups corresponds to the doublet at 1586 cm^{-1}. The peaks at 1705 cm^{-1} and 1298 cm^{-1} represent hydrogen-bonded and free carbonyl groups, respectively. A peak at 1700 cm^{-1} confirms the C=O stretching of urea groups, and the absorption at 1540 cm^{-1} corresponds to C–N stretching vibrations, validating the incorporation of MNPs into the PUU matrix.

3.3. XRD Analysis

The XRD pattern of $CoFe_2O_4$ nanoparticles shown in Figure 2 exhibits characteristic reflections at 2θ values of 19°, 30°, 35°, 43°, 53°, 57°, 63°, and 77°, corresponding to the (111), (220), (311), (400), (422), (511), (440), and (533) crystallographic planes, respectively. These peaks are consistent with the standard $CoFe_2O_4$ pattern (JCPDS Card No. 22-1086), confirming the formation of a single-phase cubic spinel structure with high crystallinity [21].
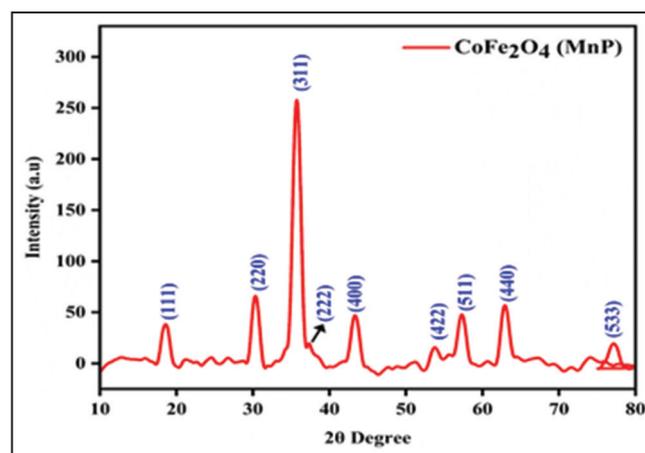
3.4. Adsorption of CV Dye

The adsorption studies using PUU/MNp employed CV, a cationic dye. Conducted adsorption experiments using a 100 mL round-bottom flask that contained 50 mL of 100 ppm CV solution and 25 mg of PUU/MNp at room temperature with constant stirring. The UV-visible spectrum exhibited a characteristic absorption peak at 590 nm, showing successful dye adsorption. Systematically evaluated various operational parameters – adsorbent dosage, initial dye concentration, contact time, and pH – to assess the PUU/MNp adsorbent performance. Table 1 provides comparative data with other polymer-based magnetic nanocomposites.

3.5. Effect of Initial Dye Concentration

Figure 3a shows the influence of initial CV concentration (10–100 ppm) on the adsorption efficiency and capacity of PUU/MNp. Increasing dye concentration decreased adsorption efficiency, likely because of saturation of active sites on the adsorbent surface. However, higher dye concentrations increased the adsorption capacity; this increase stemmed from a stronger driving force for mass transfer, allowing dye molecules to penetrate deeper into the nanocomposite structure's internal pores and active sites.

3.6. Effect of Adsorbent Dosage

Investigated the effect of PUU/MNp dosage on adsorption efficiency by varying the amount of adsorbent from 5 mg to 50 mg, using a fixed
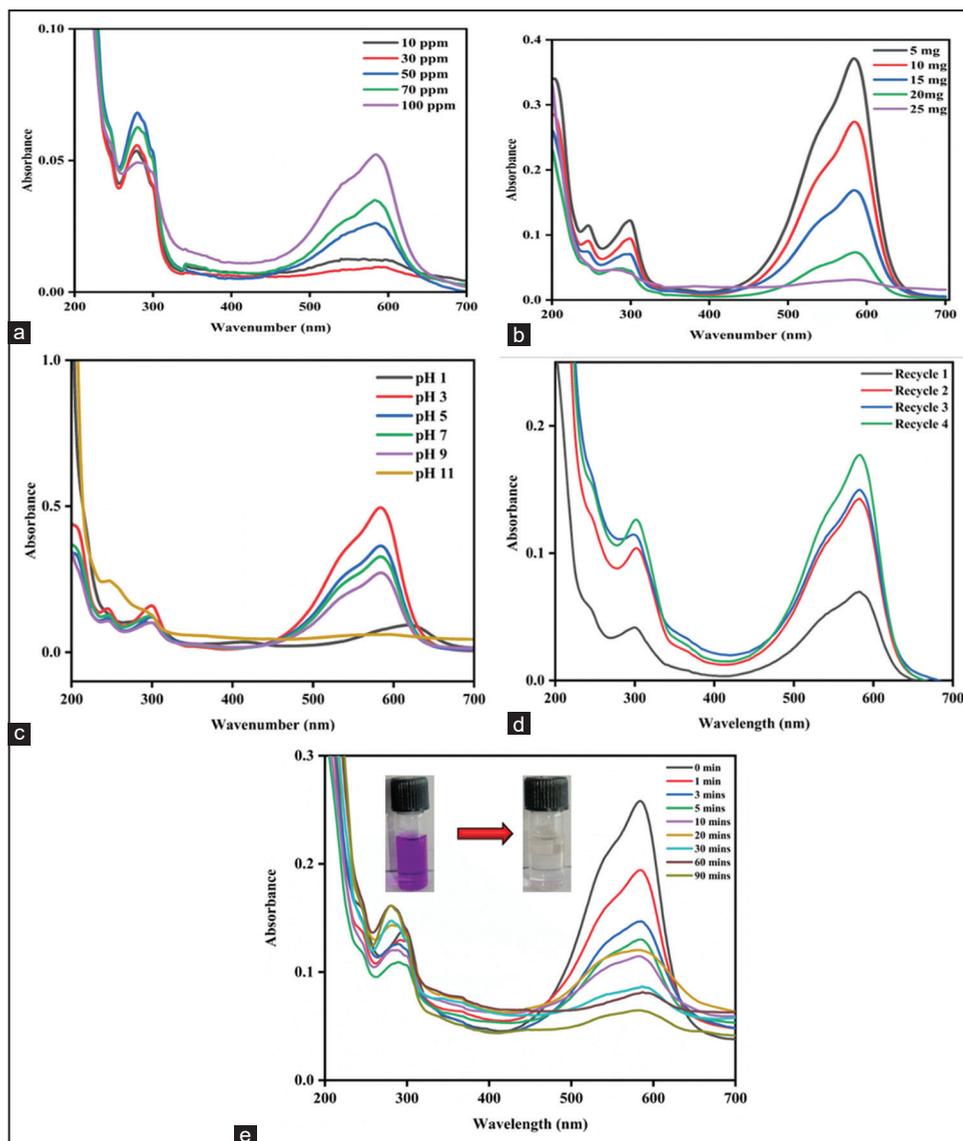
Figure 3: Effect of initial dye concentration (a), Effect of adsorbent dosage (b), Effect of pH (c), Effect of contact time (d), and Effect of recyclability (e).

CV dye concentration of 100 ppm at 30°C. As shown in Figure 3b, an increase in dosage led to enhanced dye removal efficiency, attributed to the greater availability of active sites and surface area. Beyond 50 mg, the adsorption efficiency plateaued, showing saturation. These findings led us to select 25 mg as the optimal dosage for subsequent experiments.

3.7. Effect of pH

The pH of the dye solution plays a crucial role in the adsorption process. Examined the effect of pH on CV dye adsorption by PUU/MNp across the range of pH 1–11 [Figure 3c]. At lower pH values, the adsorbent surface became positively charged because of protonation, resulting in electrostatic repulsion with the cationic dye molecules and reduced adsorption. As the pH increased, the adsorbent surface gained negative charges through OH⁻ ion adsorption, promoting electrostatic attraction with the positively charged dye species and leading to enhanced adsorption efficiency. The basic nature of CV dye (pKa = 0.8) ensured its presence as a cationic species across the tested pH range.

3.8. Effect of Contact Time

Assessed the effect of contact time on dye adsorption over 0–90 min

using a 100 ppm CV solution and 25 mg of PUU/MNp. As illustrated in Figure 3e, rapid dye adsorption occurred within the first 5 min, likely because of the abundance of available active sites. The adsorption rate slowed after 30 min, approaching equilibrium. The process has two apparent stages: An initial fast phase (5–20 min) followed by a slower phase due to site saturation and reduced mass transfer.

3.9. Recyclability Studies

Reusability is a key parameter for evaluating the economic viability and practical application of an adsorbent. Tested the recyclability of PUU/MNp over four adsorption-desorption cycles is represented in Figure 3d. The material kept considerable adsorption efficiency across cycles, demonstrating its potential for repeated use in real-time wastewater treatment applications.

4. CONCLUSION

We successfully synthesized a novel PUU/CoFe$_2$O$_4$ (PUU/MNp) nanocomposite through interfacial step-growth polymerization in mini-emulsion. Incorporating CoFe$_2$O$_4$ MNPs into the PUU matrix effectively addressed nanoparticle agglomeration, enhancing the

surface accessibility and dispersibility of the active material. The synthesized PUU/MNp exhibited excellent adsorption performance toward CV dye, achieving significant dye removal within 90 min, as confirmed by UV-visible spectroscopic analysis. The nanocomposite showed promising reusability, maintaining considerable adsorption efficiency over four successive cycles. These findings suggest that the PUU/MNp nanocomposite offers a cost-effective, magnetically retrievable, and environmentally sustainable approach for the removal of cationic dyes from aqueous environments, highlighting its potential for practical wastewater treatment applications.

5. ACKNOWLEDGMENT

6. CONFLICT OF INTEREST

The authors declared that they have no conflict of interest.

7. REFERENCES

1. M. T. Yagub, T. K. Sen, S. Afroze, H. M. Ang, (2014) Dye and its removal from aqueous solution by adsorption: A review, *Advances in Colloid and Interface Science*, **209:** 172-184.
2. V. Katheresan, J. Kansedo, S.Y. Lau, (2018) Efficiency of various recent wastewater dye removal methods: A review, *Journal of Environmental Chemical Engineering*, **6:** 4676-4697.
3. M. Liu, Q. Chen, K. Lu, W. Huang, Z. Lü, C. Zhou, S. Yu, C. Gao, (2017) High efficient removal of dyes from aqueous solution through nanofiltration using diethanolamine-modified polyamide thin-film composite membrane, *Separation and Purification Technology*, **173:** 135-143.
4. A. Roy, H. C. Ananda Murthy, H. M. Ahmed, M. N. Islam, R. Prasad, (2022) Phytogenic synthesis of metal/metal oxide nanoparticles for degradation of dyes, *Journal of Renewable Materials*, **10:** 1911-1930.
5. V. Selvaraj, T. Swarna Karthika, C. Mansiya, M. Alagar, (2021) An over review on recently developed techniques, mechanisms and intermediate involved in the advanced azo dye degradation for industrial applications, *Journal of Molecular Structure*, 1224: 129195.
6. E. Z. Wang, Y. Wang and D. Xiao, (2021) Polymer nanocomposites for photocatalytic degradation and photoinduced utilizations of azo-dyes, *Polymers (Basel)*, **13:** 1215.
7. P. Manoj Kumar Reddy, S. Mahammadunnisa, B. Ramaraju, B. Sreedhar and C. Subrahmanyam, (2013) Low-cost adsorbents from bio-waste for the removal of dyes from aqueous solution, *Environmental Science and Pollution Research*, **20:** 4111-4124.
8. N. Bao, L. Shen, Y. Wang, P. Padhan, A. Gupta. (2007) A facile thermolysis route to monodisperse ferrite nanocrystals, *Journal of the American Chemical Society*, **129:** 12374-12375.
9. Y. Zhang, L. Bai, W. Zhou, R. Lu, H. Gao, S. Zhang, (2016) Superior adsorption capacity of Fe3O4@nSiO2@mSiO2

10. core-shell microspheres for removal of congo red from aqueous solution, *Journal of Molecular Liquids*, **219:** 88-94.
10. P. E. Feuser, V. Chiaradia, N. C. Galvani, R. Scussel, R. A. Machado-de-Ávila, D. De Oliveira, P. H. Hermes de Araújo, C. Sayer, (2021) *In vitro* cytotoxicity and hyperthermia studies of superparamagnetic poly(urea-urethane) nanoparticles obtained by miniemulsion polymerization in human erythrocytes and NIH3T3 and HeLa cells, *International Journal of Polymeric Materials and Polymeric Biomaterials*, **70:** 476-485.
11. R. Jayalakshmi, J. Jeyanthi, (2018) Synthesis and structural characterization of polymer-based cobalt ferrite nanocomposite with core-shell structure, *Journal of Inorganic and Organometallic Polymers and Materials*, **28:** 1286-1293.
12. K. K. Siong, N. F. Amari, T. C. Yuan, S. Radiman, R. Yahaya, M. S. Yasir, (2013) Preparation, characterization and properties of core-shell cobalt ferrite/polycaprolactone nanomagnetic biomaterials, *Sains Malays*, **42(2):** 167-173.
13. C. I. Covaliu, C. Matei, A. Ianculescu, I. Jitaru, D. Berger, (2009) Fe3O4 and CoFe2O4 nanoparticles stabilized in sodium alginate polymer, *UPB Scientific Bulletin Series B: Chemistry and Materials Science*, **71(4):** 53.
14. A. Jazzar, H. Alamri, Y. Malajati, R. Mahfouz, M. Bouhrara, A. Fihri, (2021) Recent advances in the synthesis and applications of magnetic polymer nanocomposites, *Journal of Industrial and Engineering Chemistry*, **99:** 1-18.
15. S. Kalia, S. Kango, A. Kumar, Y. Haldorai, B. Kumari, R. Kumar, (2014) Magnetic polymer nanocomposites for environmental and biomedical applications, *Colloid and Polymer Science*, **292:** 2025-2052.
16. T. K. Mahto, A. R. Chowdhuri, S. K. Sahu, (2014) Polyaniline-functionalized magnetic nanoparticles for the removal of toxic dye from wastewater, *Journal of Applied Polymer Science*, **131(21):** 40734.
17. H. Mittal, S. B. Mishra, (2014) Gum ghatti and Fe3O4 magnetic nanoparticles based nanocomposites for the effective adsorption of rhodamine B, *Carbohydrate Polymers*, 101: 1255-1264.
18. M. Zirak, A. Abdollahiyan, B. Eftekhari-Sis, M. Saraei, (2018) Carboxymethyl cellulose coated Fe3O4@SiO2 core-shell magnetic nanoparticles for methylene blue removal: Equilibrium, kinetic, and thermodynamic studies, *Cellulose*, **25:** 503-515.
19. V. Srinivasan, V. Sumalatha, A. Prasannan, S. Govindarajan, (2022) Utilization of sulfonated waste polystyrene-based cobalt ferrite magnetic nanocomposites for efficient degradation of calcon dye, *Polymers* (*Basel*), **14:** 2909.
20. M. H. Khedr, A. A. Omar, S. A. Abdel-Moaty, (2006) Magnetic nanocomposites: Preparation and characterization of Co-ferrite nanoparticles, *Colloids and Surfaces A: Physicochemical and Engineering Aspects*, **281:** 8-14.
21. A. M. Al-Sabagh, Y. M. Moustafa, A. Hamdy, H. M. Killa, R. T. M. Ghanem, R. E. Morsi, (2018) Preparation and characterization of sulfonated polystyrene/magnetite nanocomposites for organic dye adsorption, *Egyptian Journal of Petroleum*, 27: 403-413.

Bibliographical Sketch

Dr. G. Sankar is an Assistant Professor in the Department of Polymer Science at the University of Madras, India. His research focuses on the design and development of sustainable polymeric materials, with particular expertise in polyurethanes, epoxy systems, natural polyols, and bio-based polymers. He has authored 31 research publications in peer-reviewed journals and is the inventor of a granted world patent. Dr. Sankar's work integrates fundamental polymer chemistry with application-oriented innovation, targeting advanced coatings, adhesives, elastomers, and functional materials derived from renewable resources.